

Solid Phase Synthesis of Casimersen and Its 3'-end Modification for Therapeutic Benefits

Arnab Das[†], Subhamoy Pratihar[†], Swrajit Nath Shrama[†], Jayanta Kundu^{††}, Surajit Sinha^{*†}

[†]School of Applied and Interdisciplinary Sciences, Indian Association for the Cultivation of Science, Jadavpur, Kolkata 700032

^{††} Present address: Alnylam Pharmaceuticals, Cambridge, Massachusetts 02142, United States

Phosphorodiamidate Morpholino Oligonucleotides (PMO) have been well established in the treatment of muscular dystrophies with five drugs approved so far on this scaffold. However, the literature data on synthetic methodology for PMOs is very limited in the public domain. In this report, micromole scale synthesis of PMO has been achieved with improved yield and HPLC purity. Casimersen (Amondys 45), an FDA approved drug for treatment of Duchenne Muscular Dystrophy (DMD) was selected as the standard sequence for screening various conditions. Optimization of different reaction conditions revealed that 1:1 salt of 4-cyanopyridine and methane sulphonic acid served as an efficient deblocking agent, Ramage Chemmatrix resin with sarcosine linker-loading was a suitable solid support and 1,3-Dimethyl-2-imidazolidinone (DMI) was the appropriate solvent. The compound was purified by reverse phase HPLC in Trityl ON mode and characterized by MALDI-TOF. Conjugation of PMO with stearic acid, docosanoic acid, and a phosphorothioate based linker has been shown to significantly enhance serum binding properties while avoiding adverse effects such as hemolysis or immunostimulation. These modifications not only improve the bioavailability of PMOs but also suggest potential strategies for optimizing their pharmacokinetic profiles. The minimal immune activation observed compared to traditional PMOs underscores their promising safety and efficacy in clinical applications. However, the varying rates of dialysis among different conjugates indicate a complex interaction with albumin, highlighting the need for further detailed investigation in this area.

Introduction

Oligonucleotides are being increasingly recognized as potential therapeutic agents for a variety of diseases (1). Traditional pharmaceuticals typically work by selectively binding to disease-related proteins to modulate their function. In contrast, oligonucleotides have emerged as a powerful drug modality by targeting the mRNA encoding these proteins through Watson-Crick-Franklin (WCF) pairing. Several therapies (2, 3) have been approved for the treatment of rare genetic disorders including Nusinersen (4) which has become a standard care for spinal muscular atrophy and Patisiran, a lipid-nanoparticle based siRNA drug, used for treatment of hATTR amyloidosis. A customized ASO drug Milasen has been developed to treat Batten disease, a genetic disorder unique to single pediatric patients (5). However the recent approval of Inclisiran, a GalNAc conjugated drug targeting PCSK9 for atherosclerotic heart disease and familial hypercholesterolemia in chronic cardiovascular disease marks a turning point of the field (6). In this way oligo-based therapies address the underlying causes of diseases, provide long lasting effect and offers

treatments for conditions previously considered untreatable.

Phosphorodiamidate morpholino oligonucleotides (PMO) (**Figure 1**) are unique class of antisense agents (7, 8) distinguished by their neutral inter-nucleotide linkage compared to other DNA/RNA based therapeutic agents. They can effectively inhibit gene expression by steric block mechanism (9) or mRNA splicing (10). Several FDA approved PMO based drugs are being used for the treatment of Duchenne Muscular Dystrophy (DMD). Despite their recognized importance, there are limited literature reports for an efficient synthesis method of PMOs. Gene tools LLC is the global supplier of PMOs for research purposes while Sarepta Therapeutics uses PMOs for therapeutic applications. Recently, Ajinomoto Bio-Pharma Services applied their Ajiphase technology (undisclosed) of soluble anchor based synthesis of PMO in 10 kg scale batch to support the clinical trials (11). Automated synthesis of PMOs without manual intervention has been reported by us (12)

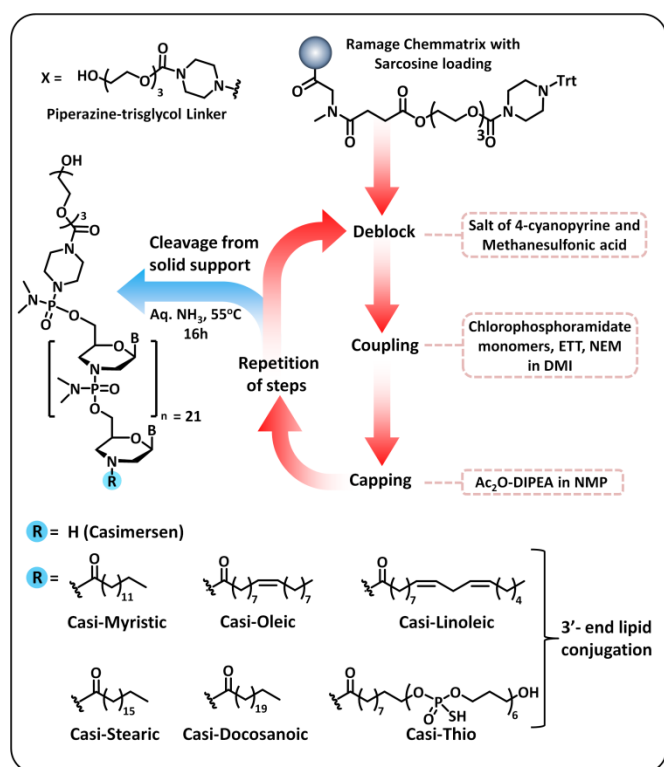


Figure 1: Chemical structure of PMO and different 3'-conjugates. (5'-X-CAATGCCATCCTGGAGTTCCTG-R-3').

and Pentelute *et. al.* (13). Additionally we (14) and Wada *et. al.* (15) reported the convenient convergent approach for synthesis of PMO, effectively eliminating (n-1) mer impurities. Apart from the H-phosphonate (16) and phosphoramidate (17) based strategy our group has recently disclosed a novel 5'-phosphoramidite based method for PMO synthesis (18). Caruthers group has reported a 3' phosphoramidite method for PMO-DNA chimera synthesis (19). In spite of having both P(V) and P(III) platforms, PMO synthesis is relatively new compared to standard phosphoramidite method of DNA/RNA synthesis and thus large-scale production methodologies in literature are lacking. The majority of currently approved synthetic therapeutic oligonucleotides are manufactured by solid phase synthesis (20). This process involves sequential addition of reactive subunits one by one to the solid support. However, the increasing number of applications in therapy presents a manufacturing challenge due to the scalability and sustainability of traditional synthesis methods. Despite these challenges, solid supported synthesis has remained the mainstream production method for

oligonucleotide drug discovery, early stage clinical investigations and commercialization for rare disease.

Herein, we report a simple and robust synthesis procedure for PMO using 10 - 15 μmol scale solid supports (**Scheme S1**). We have chosen Casimersen (Amondys 45), an FDA approved antisense oligonucleotide drug used in exon skipping therapy for DMD patients who are amenable to exon-45 skipping, as a standard for this scale-up methodology. We optimized mild deblocking agents, suitable resins with loading linker and the proper reaction conditions for a smooth and efficient linear approach to PMO synthesis. This methodology is suitable not only for lab-scale but can also be readily translated for scale-up and process management. We also conjugated different fatty acids and a newly synthesized thio-linker which can have non-covalent interaction with albumin resulting in increased blood circulation time. This conjugates were found to be non-effective towards immune activation and hemolysis.

Results and Discussion

Optimization of Deblocking Conditions. For initial optimization, polystyrene resin was chosen for the synthesis of the first 12 mer sequence of casimersen (5'-X-CAATGCCATCCT-3') and CYPTFA (salt of 3-Cyanopyridine and trifluoroacetic acid) as a deblocking agent following established report (12). The linker X of Casimersen was synthesized (Scheme 1) and loaded on solid support. Initial studies involving the synthesis of $\sim 13 \mu\text{mol}$ scale under similar conditions (12), 52.9% yield (Trityl assay) was achieved with a HPLC purity of 41% only (**Figure 2, Figure S1**). Use of CYPTFA as a deblocking agent for 10 – 15 μmol scale presented issues of heat generation during the reaction which created a lot of mist inside the reaction vessel. Use of TFA in large scale can be detrimental to oligo synthesis as it can cause depurination and strand cleavage as side reactions. Moreover, PMOs are quite acid sensitive due to their phosphorodiamidate backbone and cleaved at low pH when exposed for a long time (21). Hence an alternative was required for the repetition of the synthetic cycle.

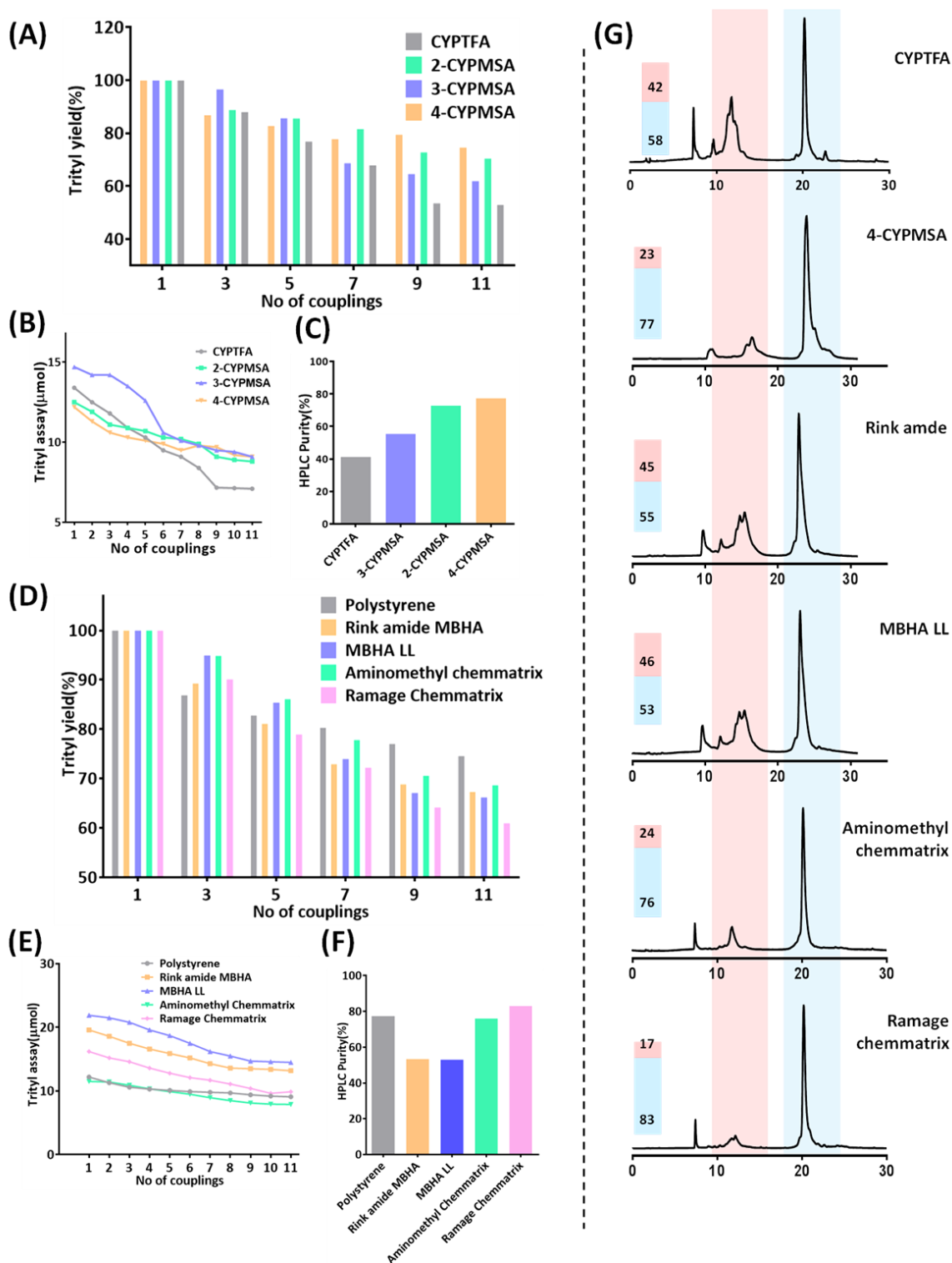


Figure 2: (A) Trityl assay (%) with different deblocking agents. (B) Trityl assay in μmol scale (C) HPLC purity of 12mer. (D) Trityl assay (%) with different solid supports. (E) Trityl assay in μmol scale (F) HPLC purity of 12 mer (5'-X-CAATGCCATCCT-3') (G) Crude HPLC chromatogram of 12-mer with different deblocking agents and solid supports. X: Piperazine-trisglycol Linker

Table 1: Optimization of deblocking agent in solid phase synthesis for efficient detritylation

Entry	Resin	Trityl assay			HPLC purity of crude (%)
		1 st Coupling (μmol)	11 th coupling (μmol)	Yield (%)	
1	3-CYPTFA (3-Cyanopyridine+TFA)	13.4	7.1	52.9	41.2
2	3-CYPMSA (3-Cyanopyridine+MSA) Concentration-2%(w/v) in 25%MeOH-DCM	14.7	9.1	61.9	55.4
3	2-CYPMSA (2-Cyanopyridine+MSA) Concentration-2%(w/v) in 25%MeOH-DCM	12.5	8.8	70.4	72.8
4	4-CYPMSA (4-Cyanopyridine+MSA) Concentration-2%(w/v) in 25%MeOH-DCM	12.2	9.2	75.4	77.4

Reagents and conditions: Resin - Polystyrene divinyl (100-200 mesh); **Deblocking** – 30s x 8 times, 1 mL each; 3-CYPTFA was prepared according to previous report; **Coupling** - 30 min x 3 times, Chlorophosphoramidate monomer concentration-0.2 M in NMP (3.2 equiv), ETT concentration (0.075M in NMP, 1.2 equiv), 4-ethylmorpholine (NEM) - 10eq, total volume≈ 200-230μL; **Sequence:** 5'-X-CAATGCCATCCT-3' (12 mer); **Linker:** X: Piperazine-trisglycol Linker.

Table 2: Optimization of solid support for synthesis of PMO

Entry	Resin	Trityl assay			HPLC purity of crude (%)
		1 st Coupling (μmol)	11 th coupling (μmol)	Yield (%)	
1	Polystyrene divinyl	12.2	9.2	75.4	77.4
2	Rink amide MBHA	19.6	13.2	67.3	53.4
3	MBHA LL	21.9	14.5	66.2	53.0
4	Aminomethyl chemmatrix	11.5	7.9	68.7	76.0
5	Ramage Chemmatrix	16.2	9.88	60.9	83.1

Reagents and conditions: **Deblocking** - 30s x 8 times, 1 mL each, 4-CYPMSA in 25%MeOH-DCM; **Coupling** - 30 min x 3 times, Monomer concentration- 0.2 M in NMP (3.2 equiv.), ETT Concentration- 0.075M in NMP (1.2 equiv.), NEM - 10 equiv. total volume≈ 200-230μL ; **Sequence:** 5'-X-CAATGCCATCCT-3'(12mer). **Linker:** X: Piperazine-trisglycol Linker (**Scheme 1**).

Table 3: Linker and reaction condition optimization

Entry	Resin	Linker	Reaction condition (in NMP)	Trityl assay			HPLC purity of crude (%)
				1 st Coupling (μmol)	11 th coupling (μmol)	Yield (%)	
1	Polystyrene	Piperazine-trisglycol	Monomer conc-0.2M (3.2 eq) ETT conc-0.075M (1.2 eq)	12.2	9.2	75.4	77.4
2	Polystyrene	Piperazine-trisglycol	Monomer conc-0.2 M (3.2eq) ETT conc-0.075 M (1.2eq) NMI conc- 0.05 M (0.5 eq)	14.2	9.4	66.1	66.4
3	Ramage Chemmatrix	Sarcosine,	Monomer conc-0.2M (3.2 eq)	15.4	11.5	74.7	80.2

		Piperazine-trisglycol	ETT conc-0.075M (1.2 eq)				
--	--	-----------------------	--------------------------	--	--	--	--

Reagents and conditions: **Deblocking-** 30s x 8 times, 1 mL each, 4-CYPMSA in 25% MeOH-DCM; **Coupling:** 30 min x 3 times, Monomer concentration -0.2M (3.2 eq), ETT concentration -0.075M (1.2eq), NEM (10 eq), total volume \approx 200-230 μ L; **Sequence:** 5'-CAATGCCATCCT-3' (12 mer).

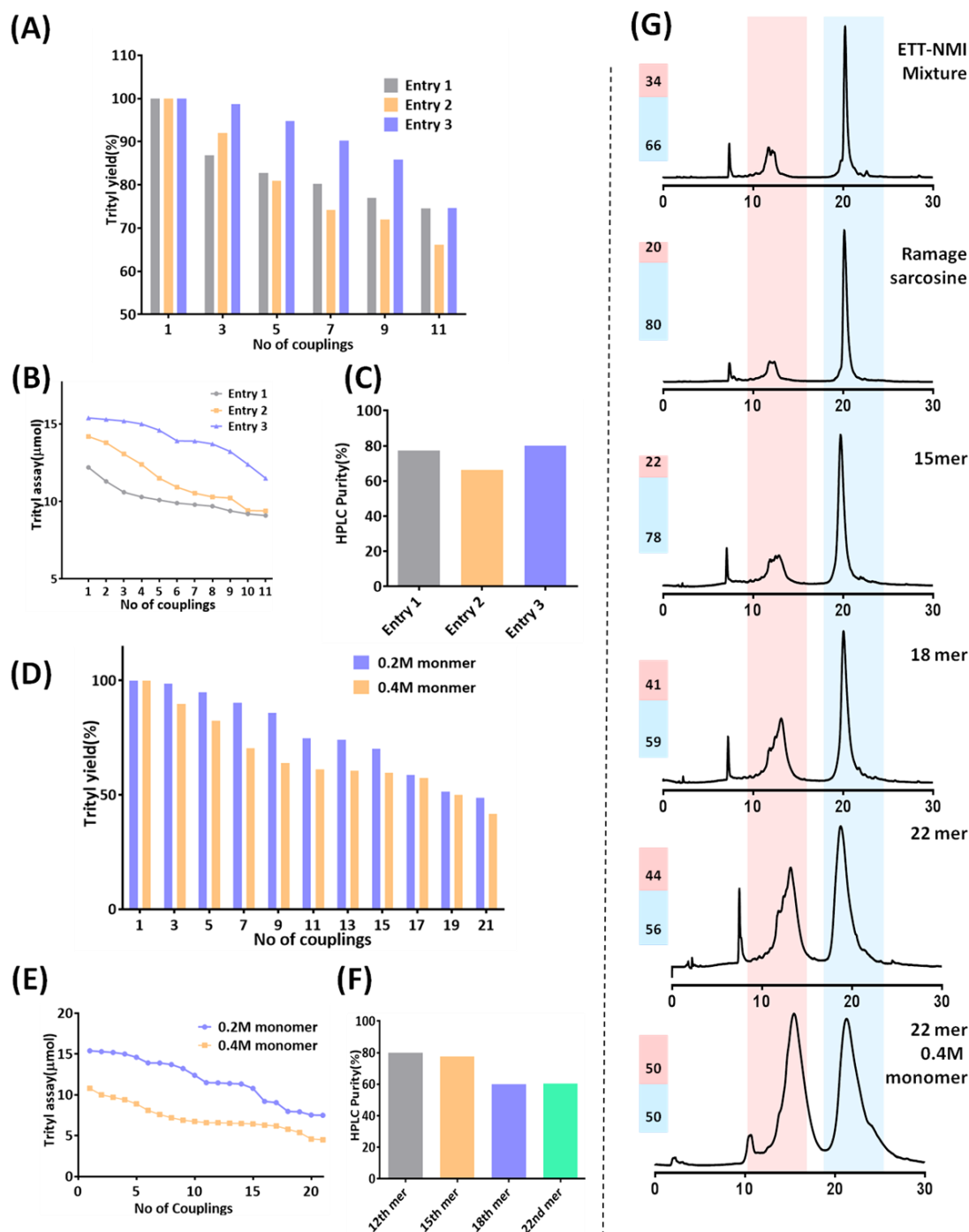


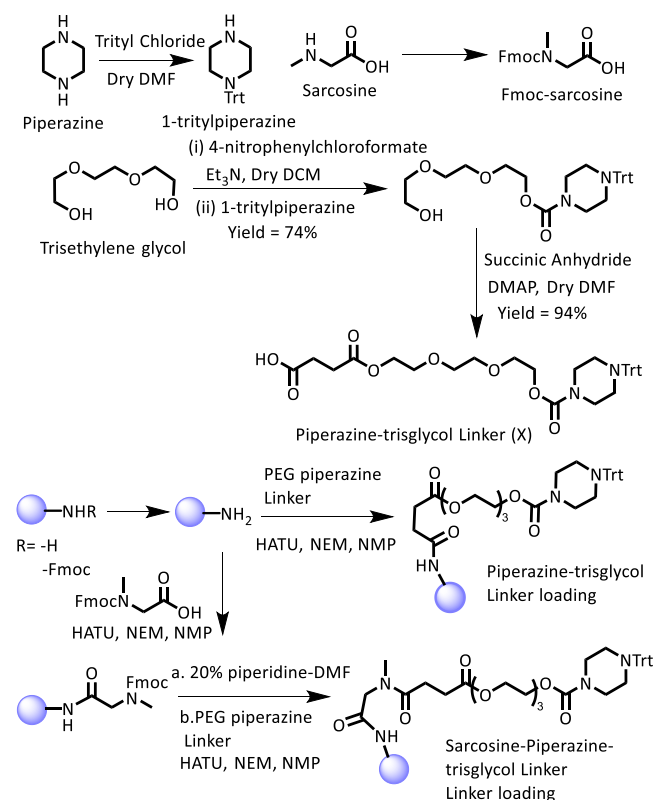
Figure 3: (A) Trityl assay (%) with different reaction condition with different linkers. (B) Trityl assay in μ mol scale (C) HPLC purity of 12mer of entries in Table 3 (D) Trityl assay (%) during full length synthesis in NMP with 0.2M and 0.4M monomer concentration. (E) Trityl assay (%) during full length synthesis in NMP with 0.2 and 0.4 (M)

monomer concentration. (F) HPLC purity of crude material at different chain length when synthesized in NMP with 0.2 M monomer concentration. (G) Crude HPLC chromatograms at different optimization steps.

Thus, we replaced TFA (pKa 0.52) with methane sulphonic (MSA) acid which has a comparatively lower acidity (pKa 1.9). We used 3-cyanopyridine along with MSA as a 1:1 salt in 25% methanol-DCM as a deblocking agent (30s x 8 times) (Figure S2). This improved the overall yield and HPLC purity of the oligo (Table 1). As we were using a salt, the conjugate acid of the cyanopyridine (MH⁺) was responsible for the removal of trityl group. Consequently, we tested the deprotection with 2 or 4- cyanopyridine (Figure S3, S4). Among these, 4-cyanopyridine demonstrated the highest efficiency with a very short deblocking time period (30s x 8 times). We proceed with 4-CYPMSA for further studies since short deblocking time is one of the necessary conditions to minimize undesired side reactions.

Optimization of Solid Support. Resin plays a crucial role during the solid phase synthesis. Its swelling properties, surface polarity, ability to diffuse reagents are key parameters for an efficient oligomer synthesis. Swelling exposes the reactive functional groups to resin surface making them available for the further coupling. The standard phosphoramidite approach uses CPG as solid support for DNA, RNA, LNA synthesis which does not have a swelling property. Since we were using chlorophosphoramidate monomers for this micromole scale synthesis, we screened various resins having good swelling properties in NMP (Figure 2, Table 2). For Rink Amide MBHA and MBHA LL resins, the average coupling efficiency was low with diminished compound purity as shown by their HPLC profiles (Figure S5, S6). In contrast, Polystyrene and Aminomethyl Chemmatrix (Figure S7) resins showed a steady progress in coupling, with HPLC purity (trityl ON) of 77.4% and 76%, respectively. Interestingly, Ramage Chemmatrix resin, despite showing a poor trityl yield, exhibited the highest HPLC purity among all tested resins (Figure S8). The lack of correlation between the trityl assay and the HPLC profile suggested that there is a loss of the material during the synthetic cycle. Although Ramage Chemmatrix resin delivered high purity, the issue of material retention efficiency needed to be resolved to enhance the overall yield.

Our initial investigations identified polystyrene and Ramage Chemmatrix as the most promising solid supports for further exploration. Polystyrene had shown a comparatively better yield of the 12 mer oligo than Ramage (60.9%). In contrast, Ramage demonstrated highest compound purity of 83.1%, a crucial factor for oligonucleotide synthesis. Consequently, we examined the reaction conditions on polystyrene support and introduced NMI (1-methyl imidazole) as an additive to facilitate the coupling (Table 3, Figure S9). NMI is known for its potential as a nucleophilic catalyst in the coupling step and has previously shown promise in Fmoc protected morpholino chlorophosphoramidate monomer synthesis (12). Despite these efforts, NMI failed to improve the yield as well as HPLC purity of the oligo on polystyrene resin. As a result, we transitioned to Ramage as the preferred solid support, given its ability to consistently deliver the highest purity of the oligo (Figure 3).



Scheme 1: Synthesis of Resin–Linker loading

Table 4: Monitoring the reaction progress during the full length synthesis

Entry	Sequence	Trityl assay			HPLC purity of crude (%)
		1 st Coupling (μmol)	Final coupling (μmol)	Yield (%)	
1	5'-X-CAATGCCATCCT-3'	15.4	11.5	74.7	80.2
2	5'-X-CAATGCCATCCTGGA-3'	15.4	10.8	70.1	77.6
3	5'-X-CAATGCCATCCTGGAGTT-3'	15.4	8.0	51.9	59.3
4	5'-X-CAATGCCATCCTGGAGTTCCTG-3'	15.4	7.5	48.7	56.2
5 ^a	5'-X-CAATGCCATCCT-3'	10.8	6.6	61.1	nd
6 ^a	5'-X-CAATGCCATCCTGGAGTTCCTG-3'	10.8	4.2	38.9	50.0

Reagents and conditions: Deblocking- 30s x 8 times, 1 mL each, 4-CYPMSA in 20% MeOH-DCM; **Coupling -** (30 min x 3 times), Monomer concentration-0.2 M in NMP (3.2 eq), ETT concentration 0.075 M (1.2 eq) in NMP, NEM (10 eq) total volume ≈ 200-230 μL.

^aMonomer concentration 0.4 M (6.4 eq), ETT-0.125 M (2.4 eq), NEM (10 eq) total volume ≈ 200-230 μL. nd-not determined.

The yield (trityl assay) was reported as the ratio of the (n-1)th coupling and 1st coupling. X: Piperazine-trisglycol Linker

Table 5: Solvent optimization for efficient coupling

Entry	Solvent	Trityl assay			HPLC purity of crude (%)	Average coupling Yield (%)
		1 st Coupling (μmol)	21 st coupling (μmol)	Yield (%)		
1	NMP	15.4	7.5	48.7	56.2	96.5
2 ^a	DMSO	11.5	nd	nd	nd	90.8
3	25% DMSO in NMP	11.4	6.8	59.6	65.6	97.5
4	DMI 1	12.4	8.8	70.9	74.3	98.3
5 ^b	DMI 2	14.5	11.2	77.2	79.4	98.7

Reagents and conditions: Deblocking 30s x 6 times, 1 mL each, 4-CYPMSA in 20 % MeOH-DCM; **Coupling-** 30 min x 3 times, Monomer concentration-0.2 M (3.2 eq), ETT-0.075 M (1.2 eq), NEM (10 eq), total volume ≈ 200-230 μL; **Sequence:** 5'-X-CAATGCCAT CCTGGAGTTCCTG-3' (22 mer). X = Piperazine-trisglycol Linker

^aupto 9 mer (5'-X-CAATGCCAT-3'). Synthesis was stopped beyond this due to very poor yield (53.6 %) with HPLC purity of 60 %.

To address the reduced yield of the 12 mer on Ramage resin support, we decided to slightly modify the linker for initial loading. Therefore, we incorporated Fmoc protected sarcosine as the first loading on the resin (**Scheme 1**). Direct loading of PEG-piperazine linker on Ramage occurred with the primary amine whereas sarcosine provided a secondary amine. This prevented the succinyl linker from cyclization on solid support (22) ensuring that the entire oligo remained anchored without any loss. Thus, incorporation of sarcosine at a very early stage improved the yield significantly

without compromising the HPLC purity (**Table 3, Entry 3**) (**Figure S10**).

Casimersen (Amondys 45) synthesis. Encouraged by these results, we proceeded for the full-length synthesis of Casimersen. The reaction was monitored by trityl assay at each coupling stage and purity of the oligo was assessed by HPLC at 15th, 18th and 22nd coupling (**Figure 3, S11, S12, S13**). A steady decrease in trityl assay was observed beyond the 15 mer synthesis likely

due to overall solvation of the oligo-anchored resin in the solvent. We also carried out a synthesis with

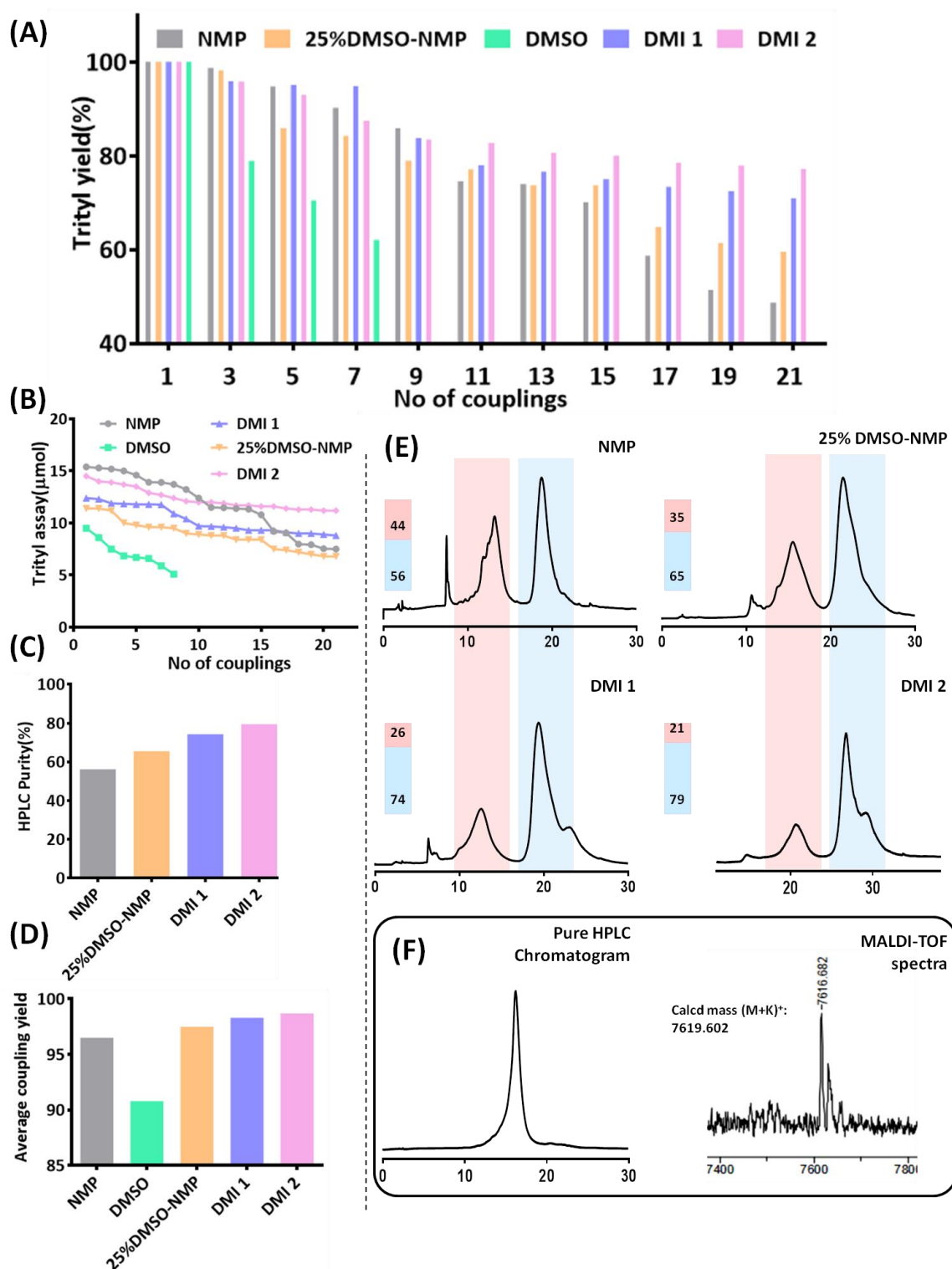


Figure 4: (A) Trityl assay (%) during full length synthesis in various solvents (B) HPLC purity of 22 mer. (C) Trityl assay in μmol scale (D) Average % coupling during per step (E) crude HPLC chromatogram with different solvents. (F) Pure HPLC chromatogram and MALDI-TOF spectra of Casimersen

increased monomer concentration on the solid support (**Table 4, Entries 5-6, Figure S14**). However, no further improvement in yield was observed either at 12 mer or at 22 mer. This may be due to increased viscosity of the reaction solvent caused by presence of high concentration of monomer and reagents leading to lower accessibility of the reaction sites.

Solvent optimization for full sequence synthesis.

Ramage chemmatrix exhibits excellent swelling properties in most of the organic solvents including acetonitrile which makes it suitable support for peptide synthesis in acetonitrile (23). However, the solvation behavior of native resin and fully protected resin bound peptide varies widely depending upon hydrogen bonding (δ) and Hildebrand solubility parameter (δ_H) with different solvents (24). These factors may contribute to reduced coupling yield during the oligomer synthesis. To address this issue, we carried out the coupling reaction in various polar aprotic solvents (**Table 5, Figure 4**). Coupling in DMSO was found to be very inefficient and we could not proceed beyond 9 mer stage (trityl yield 53%, **Figure S15**). In the presence of 25% DMSO in NMP, coupling was comparatively smoother and we completed the 22mer synthesis with 59% yield with HPLC purity of 65.6% (**Figure S16**). The use of DMI as the solvent proved to be the most effective (**Table 5, Entry 4**), demonstrating the highest yield (70.9%) with average coupling yield of 98.3% (**Figure S17**). Increasing the overall equivalency of the monomers and reaction volume gave an improved yield of 77.2% (**Figure S18**).

Then we moved for the post synthetic processing and purification (**Figure S19**) of oligo. The PMO was cleaved from the solid support and purified by HPLC on a C18 column in Trityl ON mode. Organic solvent was removed under reduced pressure and buffer was removed in 3kD MWCO centrifugal filter (Detailed discussion in **SI**). Finally, the trityl group was deblocked using 30% acetic acid in water and reaction was monitored by HPLC (**Figure S20, S21**). After quenching the acid by aqueous ammonia in ice cold condition, the reaction mixture was passed through 3kD MWCO centrifugal filter and washed repeatedly with

water. The compound was lyophilized and obtained as floppy solid. Final purity was checked by HPLC and characterized by MALDI-TOF (**Figure S21-S22**).

3'-End modification of Casimersen and their serum binding.

PMOs have not shown any notable toxicity except a reversible kidney damage (25) due to its high excretion rate (primarily through kidneys) and this was attributed to low protein binding of PMO in blood. Hence, frequent and high dosing is required for therapeutic benefit which makes the treatment exorbitantly expensive. One way to circumvent this drawback is to increase its affinity for albumin, a highly abundant plasma protein known for its extended circulatory half life due to interaction with recycling neonatal FC receptor (26). Hence it serves as a natural transport vehicle with multiple ligand binding sites making it an ideal carrier of various diagnostic and therapeutic agents (27). Our scalable strategy provides a 3'-end for the modification of Casimersen with suitable moieties which can enhance the serum binding.

Various lipophilic conjugate of oligonucleotides have been demonstrated to modulate gene-silencing and exon skipping efficacy both *in vitro* and *in vivo* (28). In this study, we conjugated various fatty acids at the 3' end of Casimersen (Casi-NH) along with a flexible thio linker as a post-synthetic modification, since it does not affect the Watson-Crick-Franklin base pairing, thereby ensuring that mRNA binding affinity remains the same. This approach has a potential to enhance the blood circulation time which can facilitate optimal biodistribution. Myristic, stearic and docosanoic acids were chosen as the saturated fatty acids for conjugation along with linoleic and oleic acid as the unsaturated congeners (**Figure 5A**). Since phosphorothioate RNAs (29) are well known for their serum binding properties, we synthesized a unique linker containing both phosphorothioate and lipophilic counterpart using 10-hydroxydecanoic acid. The acid moiety was first conjugated at the 3'-end and then standard phosphoramidite chemistry using a propane-diol based amidite was adopted to insert six phosphorothioate linkages to give Casi-Thio (**Scheme S2, Figure S23-S28, Table S1**).

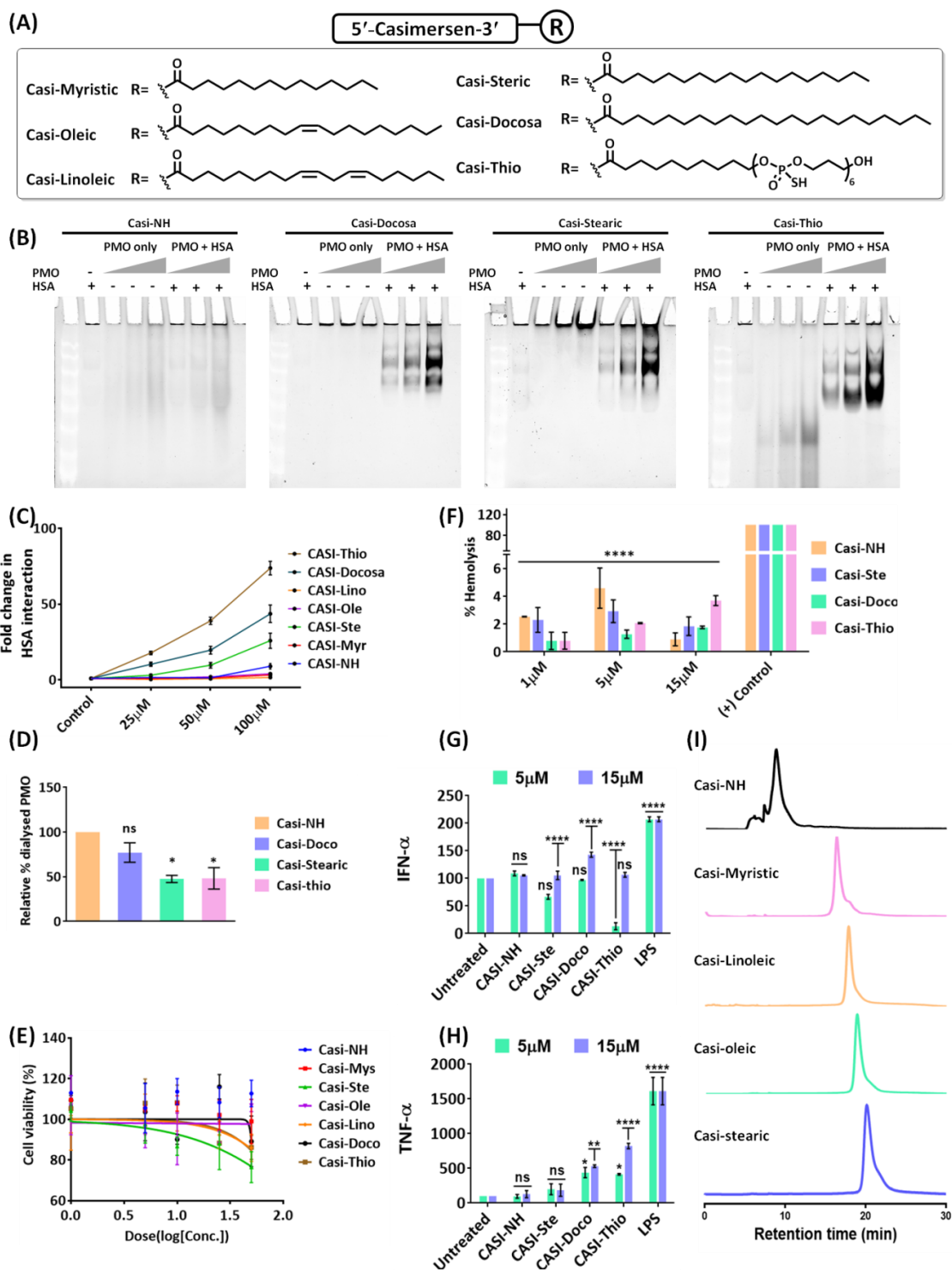


Figure 5: (A) Different functional groups conjugated at 3'-end of Casimersen. (B) Representative images of electrophoretic gel mobility assay of Casimersen, Casi-Docosa, Casi-stearic and Casi-Thio in presence of Human Serum Albumin (HSA, Conc 40mg/ml) (C) Fold change in HSA interaction of different 3'-conjugates at variable doses. n=2, Mean ± SD. (D) Relative % of dialysed PMO compared to Casi-NH (E) MTT assay of the 3'-conjugates at 1, 5, 10, 25, 50 μM doses, n=2, Mean±SD (F) Haemolytic assay of 3'-conjugates n=2, Mean±SD (G) Immune response analysis by detection of IFN-α at 5 and 15 μM in PBMCs n=2, Mean±SD (H) TNF-α level detection at 5 and 15 μM in PBMCs n=2, Mean±SD (I) Lipophilicity analysis of fatty acid conjugates.

Albumin binding by gel shift assay. The Casimersen conjugates were incubated with human serum albumin (40 mg/ml, ~600 μ M) to evaluate their binding properties. Among these modifications, Casi-Stearic, Casi-Docosa and Casi-Thio exhibited most effective serum binding demonstrating ~26%, ~44% and ~74% increased affinity, respectively compared to control as observed in electrophoretic gel mobility assay. In contrast, Casi-Myristic, Casi-Linoleic and Casi-Oleic showed poor affinity for albumin under similar conditions (**Figure 5B, 5C, S29**).

Equilibrium dialysis. Non-covalent binding of PMOs with albumin possesses significant potential to enhance bioavailability, leading to reduced renal clearance (30). Therefore, we also conducted equilibrium dialysis (31) of these PMO conjugates in the presence of human serum albumin (HSA) after the gel shift assay. For dialysis, we selected the PMO incubation dose of 100 μ M with HSA at the biologically relevant concentration (40 mg/ml, ~600 μ M) and quantified the amount of dialyzed PMO across the 20 kDa barrier using UV-visible spectroscopy. Interestingly, despite its high affinity for albumin, the docosanoic acid-conjugated PMO exhibited a higher degree of dialysis compared to the stearic and thio-conjugated PMOs (**Figure 5D**), both of which showed significance retention with HSA.

Toxicity analysis by MTT assay. We also conducted MTT assay to assess the toxicity of these lipid and thio conjugates. The study showed approximately ~76%, ~89% and ~86% of cell survivability upon treatment with stearic, docosanoic and thio linker conjugated PMOs, respectively compared to regular Casimersen in HEK-293 cell line. None of the conjugates showed any significant toxicity. The high dose tolerance with high cell viability observed with Casi-Thio can be attributed to its fewer phosphorothioate linkages (six PS-linkages) compared to the full-length PS-oligomers (**Figure 5E**). These results indicate promisingly low cytotoxicity profiles for these conjugates, supporting their potential suitability for further therapeutic development.

Hemolytic assay. In the context of exon skipping therapies, antisense agents are administered intravenously and come into direct contact with blood.

CPP-lipid conjugates have exhibited varying degrees of membrane interaction depending on their chain lengths (32). Therefore, understanding the impact of these compounds on red blood cells (RBCs) is crucial, as hemolysis of blood cells could indicate potential toxicity. In this study, we compared Casi-Stearic, Casi-Docosa, and Casi-Thio with Casi-NH against human RBCs using a hemolytic assay. We treated the RBCs with doses of 5, 10, and 15 μ M and monitored the samples over a 6-hour period. Remarkably, when compared to Casimersen, none of the Casi-long chain conjugates (Casi-Stearic, Casi-Docosa, and Casi-Thio) exhibited significant hemolysis (**Figure 5F**). This finding suggests that the conjugation of long-chain fatty acids and the thio linker does not confer hemolytic characteristics to the principal drug molecule, Casimersen.

Immunoresponse assay by ELISA. A notable characteristic distinguishing PMOs from other oligonucleotide-based drug families is their lack of immune activation (33). In contrary, phosphorothioate antisense oligonucleotides are well recognized for their immune response, typically in a sequence-dependent manner. This immune activation can be mitigated by substituting the phosphorothioate linkage (e.g., with mesyl phosphoramidate) reducing non-specific interactions with proteins on immune cells (34). To check the immune response of the PMO-fatty acid conjugated compounds and the thio-linker, peripheral blood mononuclear cells (PBMCs) were selected as the model system due to their heterogeneous population of immune cells with diverse functions. IFN- α , a type I interferon induced by long double-stranded RNA and predominantly produced by plasmacytoid dendritic cells (pDCs), was chosen to assess immune activation. TNF- α , an inflammation marker primarily secreted by monocytes, was also included in the evaluation. We chose 5 and 15 μ M dose for the immune response study to maintain parity with the earlier haemolytic assay. It has been demonstrated earlier that 10 μ M dose of PMO is sufficient for uptake in PBMCs (35). Stearic and docosanoic acid conjugates showed relatively lower immune response compared to Casimersen at low dose. However, at high dose, the IFN- α level increased for both Casi-Docosa and Casi-Thio (**Figure 5G**). This result reflected a varied immune response to the 3'-

modifications. On the other hand, the TNF- α level increased in a dose dependent manner and significant response was observed for docosanoic acid and thio linker conjugates mainly (Figure 5H). Although Casi-Stearic exhibited significant serum binding, its immunostimulatory effect was minimal compared to previous findings and comparable to regular PMO. While these preliminary results provide insights into the immune activation of PMO conjugates, future research could further explore the complex receptor-mediated pathways involved in these interactions.

Conclusions

In conclusion, this study has made significant strides in advancing the synthetic methodology for Phosphorodiamidate Morpholino Oligonucleotides (PMOs), critical in the treatment of muscular dystrophies. Using Casimersen, an FDA-approved PMO for DMD, as our standard sequence, we systematically optimized the reaction conditions to obtain casimersen (Amondys 45) 4.4 μ mol (35.4 mg) from 15.3 μ mol loading. The use of a 1:1 salt of 4-cyanopyridine and methane sulfonic acid as a deblocking agent, Ramage Chemmatrix resin with sarcosine linker-loading as a solid support, and 1,3-Dimethyl-2-imidazolidinone (DMI) as a solvent played pivotal role in enhancing synthetic efficiency. This robust and efficient protocol for PMO synthesis in micromole scale is suitable for laboratory use and readily scalable for industrial production. This methodology not only enhances the production efficiency of PMOs but also maintains high purity and yield, addressing a critical need in this field. Moving forward, this optimized synthetic approach opens doors for exploring new PMO sequences and modifications, potentially leading to improved treatments for genetic disorders. Our study also highlights several key findings regarding the modification and evaluation of PMO conjugates for therapeutic applications. We demonstrated that conjugation with fatty acids such as stearic, docosanoic acid, and a thio linker can significantly enhance serum binding properties without inducing substantial hemolysis or immunostimulation. These modifications not only improve the bioavailability of PMOs by reducing renal clearance through non-covalent binding with albumin but also suggest potential avenues for optimizing their

pharmacokinetic profiles. Furthermore, our investigation into the immunostimulatory effects of these conjugates revealed minimal immune activation compared to traditional PMOs, indicating their potential safety and efficacy for clinical applications. However, the varying extents of dialysis observed among different conjugates underscore the complexity of their interaction with albumin, suggesting the need for further elucidation of their binding mechanisms. Overall, our findings support the development of PMO conjugates as promising candidates for exon skipping therapies. Continued research efforts will be essential to refine their therapeutic potential and ensure their safety for future clinical use.

Author Contributions

S.S. supervised the complete project. A.D. performed the oligomer synthesis in micromole scale and EMSA. S.P. performed chlorophosphoramidate monomer synthesis, purification of oligomer. J.K. performed on initial Trityl-deprotection. S. N. S. performed the biophysical assays (ELISA, haemolytic assay, MTT assay, membrane dialysis). All authors have contributed to the preparation of the manuscript.

Conflicts of interest

There are no conflicts to declare.

Acknowledgements

S.S. thanks Department of Science and Technology (DST), New Delhi, Government of India (DST/TDT/TC/RARE/2022/10c2) for grant support and the TRC facility at IACS for the use of a DNA synthesizer. A.D., S.N.S., S.P., J.K. acknowledge Dr. Shalini Gupta for critical reading of the manuscript and technical assistance.

Notes and references

1. M. Egli, M. Manoharan, *Nucl. Acid Res.* 2023, **51(6)**, 2529–2573; (b) M. C. Lauffer, W. v. Roon-Mom, A. Aartsma-Rus., *Commun. Med.* 2024, **4:6**, 1-11. (c) J. Kim et al., *Nature*, 2023, **619**, 828–836.

2. A. Aartsma-Rus, and D. R. Corey. *Nucleic Acid Ther.* 2020, **30**(2), 67–70. (b) J. Scharner and I. Aznarez. *Mol. Ther.* 2021, **29**, 540-554.
3. A. Bigica, “Viltolarsen Approved for Duchenne Muscular Dystrophy Treatment.” NeurologyLive website. 12 August 2020. <https://www.neurologylive.com/view/viltolarsen-approved-for-duchenne-muscular-dystrophy-treatment>.
4. Biogen. SPINRAZA. Accessed 23 September 2020. <https://www.spinraza.com>
5. J. Kim, C. Hu, C. Moufawad El Achkar et. al., *N Engl J Med*, 2019, **381**(17), 1644–1652.
6. K. K. Ray, R. S. Wright, D. Kallend et. al., *N Engl J Med*, 2020, **382**(16), 1507–1519.
7. J. E. Summerton, D. Weller, *Antisense Nucleic Acid Drug Dev.*, 1997, **7**, 187–195.
8. J. Summerton, *Biochim. Biophys. Acta-Gene Struct. Expression*, 1999, **1489** (1), 141–158.
9. A. Nasevicius, and S. C. Ekker, *Nat. Genet.* 2000, **26**(2), 216–220.
10. P. Sazani, and R. Kole, *J. Clin. Invest.*, 2003, **112**(4), 481–486.
11. R. Obexer, M. Nassir, E. R. Moody, P. S. Baran, & S. L. Lovelock. *Science*, 2024, **384**(6692), eadl4015.
12. J. Kundu, A. Ghosh, U. Ghosh, A. Das, D. Nagar, S. Pattanayak, A. Ghose, S. Sinha, *J. Org. Chem.* 2022, **87**(15), 9466–9478.
13. C. Li, A. J. Callahan, M. D. Simon, K. A. Totaro, A. J. Mijalis, K.-S. Phadke, G. Zhang, N. Hartrampf, C. K. Schissel, M. Zhou, H. Zong, G. J. Hanson, A. Loas, N. L. B. Pohl, D. E. Verhoeven, B. L. Pentelute, *Nat. Commun.*, 2021, **12**, 4396.
14. A. Banerjee, A. Das, A. Ghosh, A. Gupta, S. Sinha, *J. Org. Chem.*, 2024, **89**(5), 2895- 2903.
15. T. Tsurusaki, K. Sato, H. Imai, K. Hirai, D. Takahashi, T. Wada, *Sci. Rep.* 2023, **13**(1), 12576.
16. J. Bhadra, J. Kundu, K. C. Ghosh, S. Sinha, *Tetrahedron Lett.*, 2015, **56**, 4565–4568.
17. J. Kundu, U. Ghosh, A. Ghosh, S. Pattanayak, A. Das, S. Sinha, *Curr. Protoc. Nucleic Acid Chem.*, 2023, **3**, 1–25.
18. (a) A. Ghosh, A. Banerjee, B. Das, S. Sinha. ChemRxiv, **2024**, DOI 10.26434/chemrxiv-2024-213qg. (b) A. Ghosh, A. Banerjee, S. Gupta, S. Sinha. *J. Am. Chem. Soc.* **2024**, *146*, 32989–33001
19. M.H. Caruthers, S. Paul, U.S. Patent 2022, 11,230,565 B2.
20. D. Altevogt, I. Cedillo, C. Curtis, L. J. Diorazio, J. Faber, M. T. Jones,... & C. Wetter, *Org. Process Res. & Dev.*, 2023, **27**(12), 2211-2222.
21. A. Ghosh, M. Akabane-Nakata, J. Kundu, J. M. Harp, M. Madaoui, M. Egli,... & S. Sinha, *Org. Lett.*, 2023, **25**(6), 901-906.
22. (a) Y. Palom, A. Grandas, & E. Pedroso, *Nucleosides & Nucleotides*, 2006, **17**(7), 1177-1182. (b) S. Perez-Rentero, J. Alguacil, & J. Robles, *Tetrahedron*, 2009, **65**(6), 1171-1179.
23. G. A. Acosta, M. del Fresno, M. Paradis-Bas, M. Rigau-DeLlobet, S. Cote, M. Royo, & F. Albericio, *J. Pep. Sci.*, 2009, **15**(10), 629-633.
24. C. K. Taylor, P. W. Abel, M. Hulce, & D. D. Smith, *J. Pept Res.*, 2005, **65**(1), 84-89.
25. (a) K. R. Q. Lim, R. Maruyama, & T. Yokota. *Drug design, development and therapy*, 2017, 533-545. (b) P. Andersson et. al., *Nucleic Acid Ther.* 2023, DOI: 10.1089/nat.2022.0061. (c) P. Sazani et. al., *J. Neuromuscul. Dis.*, 2016, **3**, 381-393
26. M. T. Larsen, M. Kuhlmann, M. L. Hvam, & K. A. Howard., *Mol. Cell Ther.*, 2016, **4**, 1-12.

27. B. Elsadek, & F. Kratz., *J. Controlled Release*, 2012, **157**(1), 4-28.
28. (a) M. E. Østergaard, M. Jackson, A. Low, A. E. Chappell, R. G. Lee, R. Q. Peralta,... & P. P. Seth., *Nucleic Acids Res.*, 2019, **47**(12), 6045-6058. (b) E. Marchesi, R. Cortesi, L. Preti, P. Rimessi, M. Sguizzato, M. Bovolenta, & D. Perrone, *Int. J. Mol. Sci.*, 2022, **23**(8), 4270. (c) A. Biscans, J. Caiazzi, N. McHugh, V. Hariharan, M. Muhuri, & A. Khvorova, *Mol. Ther.*, 2021, **29**(4), 1382-1394. (e) H. H. Fakih, Q. Tang, A. Summers, M. Shin, J. E. Buchwald, R. Gagnon,... & H. F. Sleiman, *Mol. Ther. Nucleic Acids*, 2023, **34**. (e) A. E. Felber, N. Bayó-Puxan, G. F. Deleavey, B. Castagner, M. J. Damha, & J. C. Leroux. *Biomaterials*, 2012, **33**(25), 5955-5965. (f) Craig L. Duvall et. al. *Nat. Commun.*, 2024, **15**, 1581 <https://doi.org/10.1038/s41467-024-45609-0>.
29. M. Hyjek-Składanowska, T. A. Vickers, A. Napiórkowska, B. A. Anderson, M. Tanowitz, S. T. Crooke, ... & M. Nowotny, *J. Am. Chem. Soc.*, 2020, **142**(16), 7456-7468.
30. M. Dirin, J. Winkler. *Expert Opin. Biol. Ther.*, 2013, **13**(6), 875-888.
31. A. Plum, L. B. Jensen, & J. B. Kristensen. *J. Pharm. Sci.*, 2013, **102**(8), 2882-2888.
32. T. Lehto, L. Vasconcelos, H. Margus, R. Figueroa, M. Pooga, M. Hällbrink, & U. Langel, *Bioconjugate Chem.*, 2017, **28**(3), 782-792.
33. E. Kaye, J. Mendell, L. Rodino-Klapac, Z. Sahenk, L. Lowes, L. Alfano, K. Berry, A.G. Ramirez, S. Lewis, K. Flanigan, L. Cripe, S. Al-Zaidy, P. Duda, P. Sazani, J. Saoud, *Neuromuscul. Disord.* 2015, **25**, S263.
34. B. A. Anderson, G. C. Freestone, A. Low, C. L. De-Hoyos, W. J. D. Iii, M. E., Østergaard,... & P. P. Seth. *Nucleic Acids Res.*, 2021, **49**(16), 9026-9041.
35. P. L. Iversen, K. M. Aird, R. Wu, M. M. Morse, G. R. Devi, *Curr. Pharm. Biotechnol.*, 2009, **10**(6), 579-588.